Estimating the Expressed Temperature and Fractional Area of Hot Lava at the Kilauea Vent with AVIRIS Spectral Measurements

Robert O. Green
Jet Propulsion Laboratory, California Institute of Technology, Pasadena, California 91109

INTRODUCTION

Imaging spectroscopy offers a framework based in physics and chemistry for scientific investigation of a wide range of phenomena of interest in the Earth environment. In the scientific discipline of volcanology knowledge of lava temperature and distribution at the surface provides insight into the volcano status and subsurface processes. A remote sensing strategy to measure surface lava temperatures and distribution would support volcanology research. Hot targets such as molten lava emit spectral radiance as a function of temperature. Figure 1 shows a series of Planck functions (Liou, 1980) calculated radiance spectra for hot targets at different temperatures. A maximum Lambertian solar reflected radiance spectrum is shown as well. While similar in form, each hot target spectrum has a unique spectral shape and is distinct from the solar reflected radiance spectrum. Based on this temperature-dependant signature, imaging spectroscopy provides an innovative approach for the remote-sensing-based measurement of lava temperature. A natural site for investigation of the measurement of lava temperature is the Big Island of Hawaii where molten lava from the Kilauea vent is present at the surface. Figure 2 shows a satellite image of Hawaii with the vent location identified.

On April 26, 2000 the Airborne Visible/Infrared Imaging Spectrometer (AVIRIS) (Green et al., 1998) measured the active volcanic vent on the Big Island of Hawaii. Figure 3 shows the AVIRIS image of the vent. AVIRIS measures spectra from 400 to 2500 nm with nominally 10-nm sampling and response function full-width-at-half maximum. These spectra are acquired as images with a width of 11 km and length of up to 800 km from the Q-bay of the ER-2 aircraft platform flying at 20 km altitude. AVIRIS spectral images are spectrally, radiometrically, and spatially calibrated (Chrien et al., 1990, 1995, 1996, 2000).

In the past, AVIRIS data sets have been used for the analysis of hot volcanic targets (Oppenheimer et al., 1993) and hot burning fires (Green, 1996). The research presented here builds upon and extends this earlier work. The year 2000 Hawaii AVIRIS data set has been analyzed to derive lava temperatures taking into account factors of fractional fill, solar reflected radiance, and atmospheric attenuation of the surface emitted radiance. The measurements, analyses, and current results for this research are presented here.

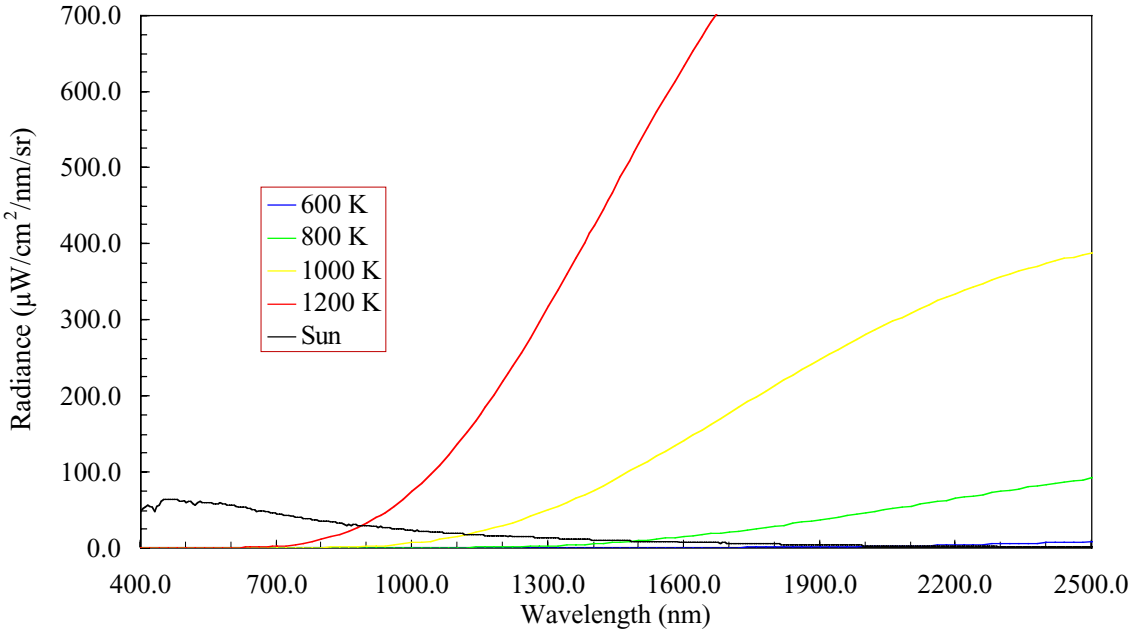

Figure 1. Maximum Lambertian reflected solar radiance spectrum as well as the emitted radiance spectra from the Planck function at temperatures of 600, 800, 1000, and 1200 K.

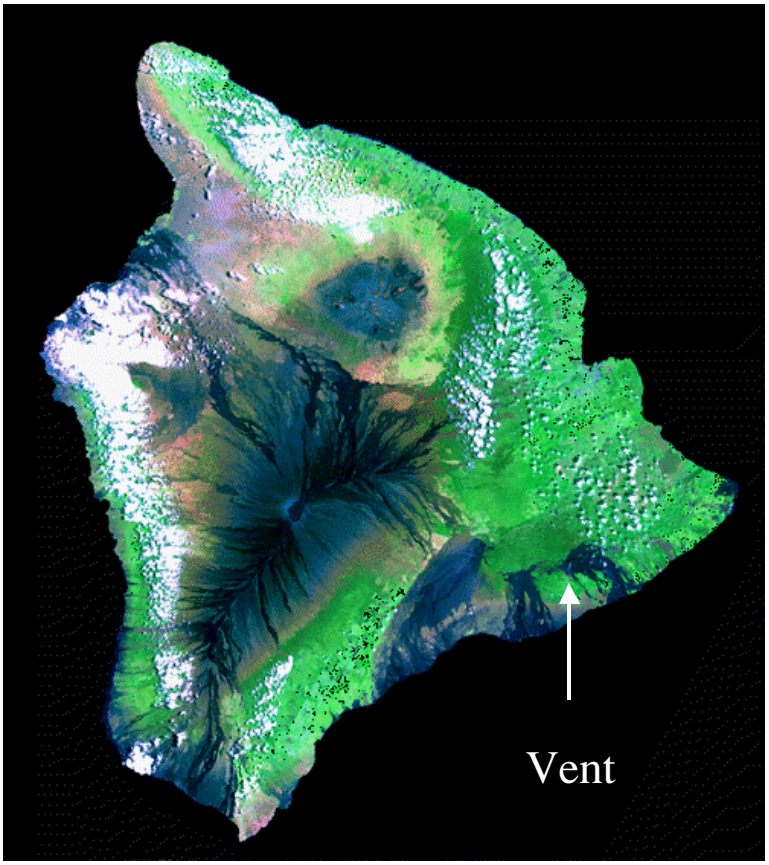

Figure 2. Image of Hawaii acquired by 1-km multispectral satellite sensor showing the location of the active volcanic vent on the Big Island of Hawaii.

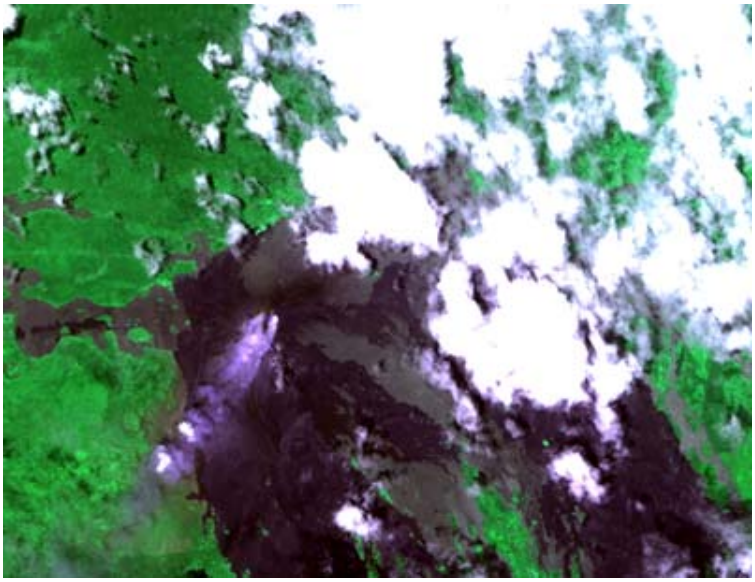

Figure 3. AVIRIS image of the active volcanic vent on Hawaii acquired on April 26, 2000.

AVIRIS MEASUREMENTS

The AVIRIS instrument imaged the active vent on the Big Island of Hawaii April 26, 2000. The complexity of the spectral signatures of a hot lava target and other Earth environment components is revealed through the different wavelength images of the AVIRIS data set. Figure 4 shows the AVIRIS image measured at 500.4 nm in the solar reflected spectrum. This image shows the volcanic plume exiting from the vent, surface rock, and dark vegetation features, as well as an extensive field of bright water vapor clouds. Figure 5 shows an image at 1503.4 nm wavelength. At this wavelength the plume is less opaque and bright spots at the surface are apparent. These high intensity spots near the source of the plume are an indication that radiance emitted by the lava is being measured by AVIRIS. Vegetation is consistently brighter than the rock cover surface near the active vent. The water vapor clouds are bright and dominate the image. In Figure 6 the AVIRIS image measured at 2500.9 nm is shown. At this wavelength the plume is largely transparent, and seven high intensity hot spots are evident near the source of the plume. These hot spots are sources of emitted radiance and are the highest intensity components of the image at this wavelength. The signal levels for the solar reflected radiance from the surface and clouds components are low due to the strong attenuation by atmospheric water vapor.

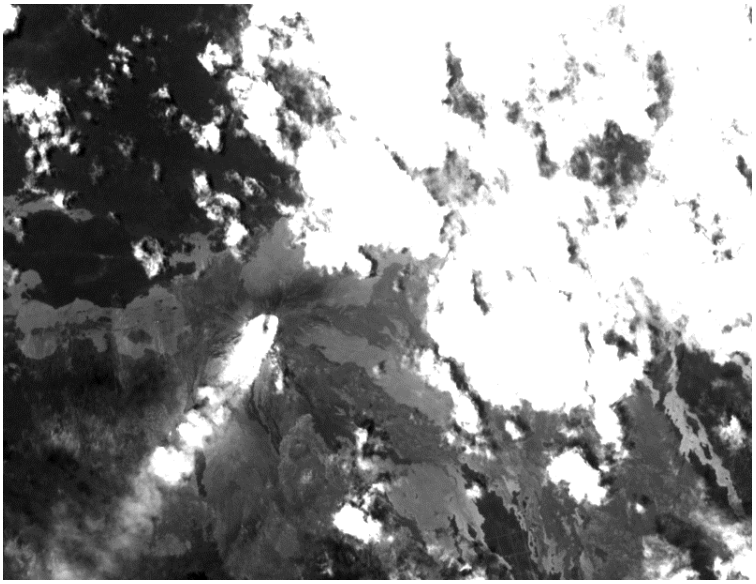

Figure 4. AVIRIS image from 500.4 nm showing solar reflected radiance from the region including the active volcanic vent.

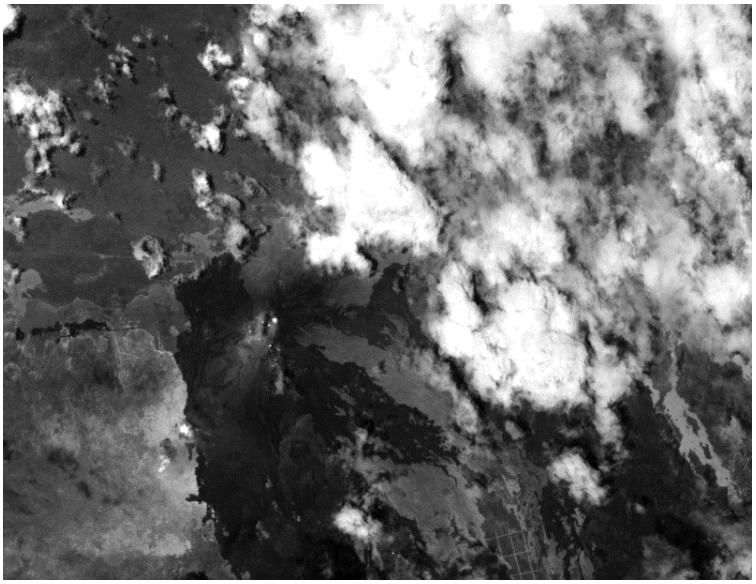

Figure 5. AVIRIS image at 1503.4˚nm showing mixture of solar reflected radiance and hot target radiance from the active volcanic vent.

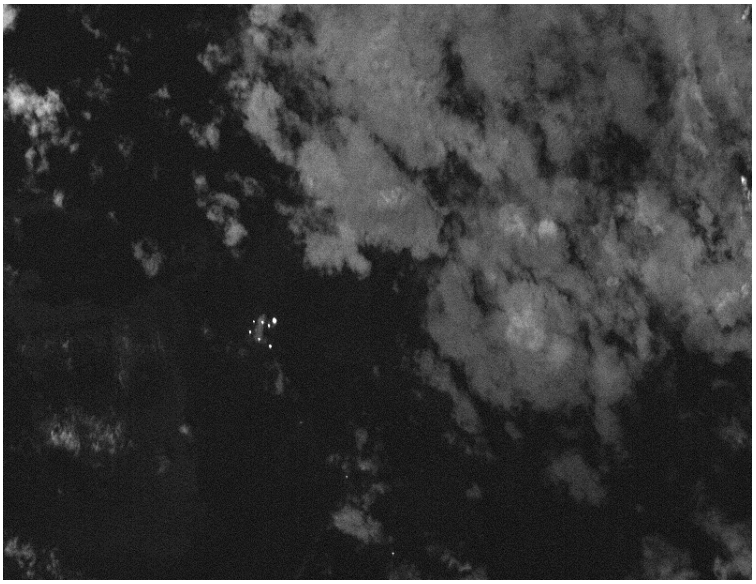

Figure 6. AVIRIS image at 2500.9 nm showing the emitted radiance of the hot lava.

In addition to the image perspective, the AVIRIS data set allows examination of the contiguous spectral signature of each measured spatial element in the image. Figure 7 shows selected spectra from the data set. Absorption and scattering effects due to the atmosphere are present in each spectrum. The dominant atmospheric absorber is water vapor with significant absorption bands at 940, 1150, 1400, 1900, and 2600 nm. The vegetation spectrum shows the chlorophyll absorption in the range 400 to 700 nm, high radiance levels from 750 to 1350 nm, and low intensity from 1350 to 2500 nm. The rock surface shows a comparatively uniform low radiance signal across the spectral range. In contrast, the cloud is bright across the spectral range. The hot lava spectrum has a form similar in shape to the cloud from 400 to 1000 nm. Beyond 1000 nm, the spectral radiance signature increases until the AVIRIS dynamic range saturates near 2000 nm. In the 1450 to 2500 nm portion of the spectrum, the emitted radiance from the hot lava target dominates the spectral signature. The distinct intensity and shape of this emitted spectral radiance provides the basis for lava temperature and fractional area estimation.

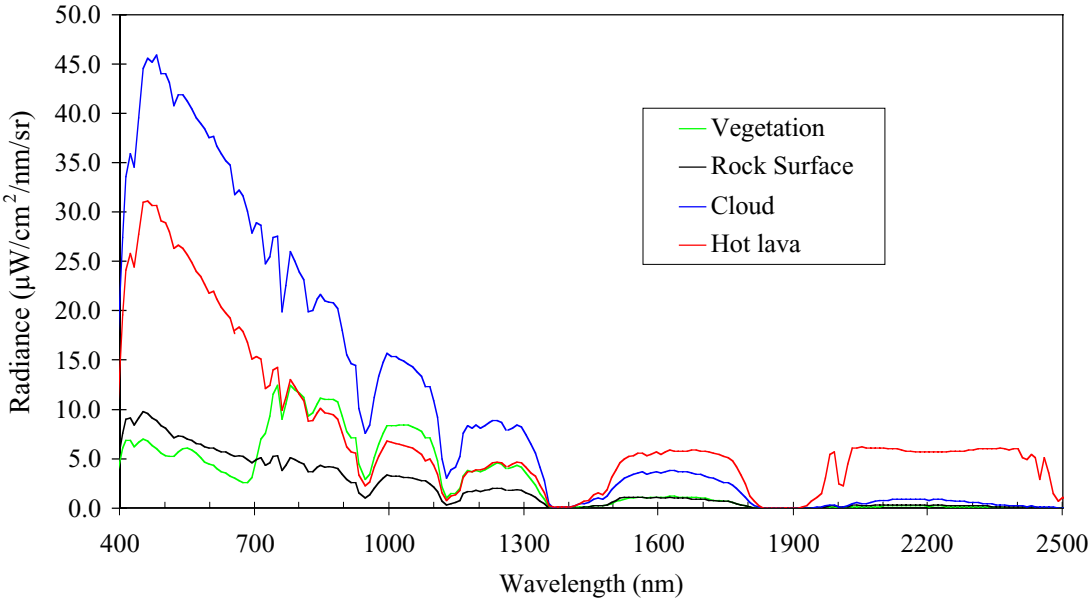

Figure 7. AVIRIS spectra spanning the range of major spectral signatures in the April 26, 2000 volcanic vent data set. At 2000 nm AVIRIS is saturated by emitted radiance over the hot lava target.

TEMPERATURE ANALYSIS

For the AVIRIS Hawaii data set, seven hot spots were analyzed to determine the expressed lava temperature and fractional area. Figure 8 shows an image with these seven targets labeled A through G. From each hot spot, the spectrum with the highest radiance from 1200 to 2500 was extracted for analysis. These extracted radiance spectra include effects from the solar source, the atmosphere, the surface, and the exposed hot lava. Equation 1 gives a simplified expression for the total radiance measured by AVIRIS over a hot target. In this equation L_t is the radiance measured by AVIRIS, I_0 is the exoatmospheric solar irradiance, ρ_a is the atmospheric reflectance, T_d is the downward transmittance, ρ_s is the surface reflectance, T_u is the upward transmittance, F_1 is the fractional area of the hot target, and B_{t1} is the Planck function radiance emitted for a given temperature. All quantities are for the illumination and observation geometry of the measurement at each wavelength across the AVIRIS spectral range.

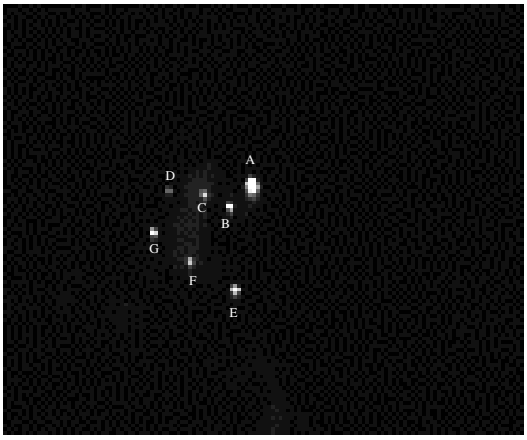

Figure 8. Location of hot spots near volcanic vent on April 26, 2000.

The approach for temperature estimation with the extracted AVIRIS spectra is based upon the Planck function. The Planck function allows direct calculation of the spectral distribution of radiance for a target of a given temperature and unity emissivity. For each AVIRIS hot target spectrum, an adjacent cool surface spectrum was identified that best matched the hot spectrum in the range from 400 to 1000 nm. This cool spectrum was used to assess and suppress the atmospheric radiance and surface reflected radiance in the hot target spectrum. Figure 9 shows the hot spectrum, adjacent cool spectrum, and difference spectrum for hot spot A. The resulting difference spectrum is dominated by the hot lava emitted radiance. Effects of atmospheric transmittance from the surface to AVIRIS are still present as well as saturation of the AVIRIS dynamic range beyond 1500 nm. For this initial analysis, a Planck function model with parameters temperature and fractional area fill was fit to the AVIRIS difference spectrum only in the spectral regions of high atmospheric transmittance and unsaturated data. Figure 10 shows a temperature and area estimation result from this analysis for hot spot A with a temperature of 908 K and fractional area fill of 0.068. The analysis was repeated for the seven extracted hot spot spectra. Figures 11 and 12 give the temperature and fractional area fill results for hot spots C and E, respectively. A temperature of 1239 K and 0.0016 fractional fill was derived for hot spot C and 1067 K and 0.025 fractional fill for hot spot E. Hot spot C had the highest derived temperature and yet due to a low fractional fill did not saturate in any portion of the AVIRIS spectral range. Hot spot E saturated the AVIRIS dynamic range in portions of the spectrum beyond 2000 nm. A summary of the temperatures and area fraction derived for each of the hot spots analyzed is given in Table 1. The temperatures range from 908 K to 1204 K and fractional areas from 0.0016 to 0.24. This simple algorithm of Equation 1 demonstrates the leverage of imaging spectrometer measurements for derivation temperature and fractional fill areas estimates for hot targets on the surface of the Earth.

$$L_t = I_0\rho_a/\pi + I_0T_d\rho_sT_u/\pi + F_1B_{t1} \qquad \text{Equation 1}$$

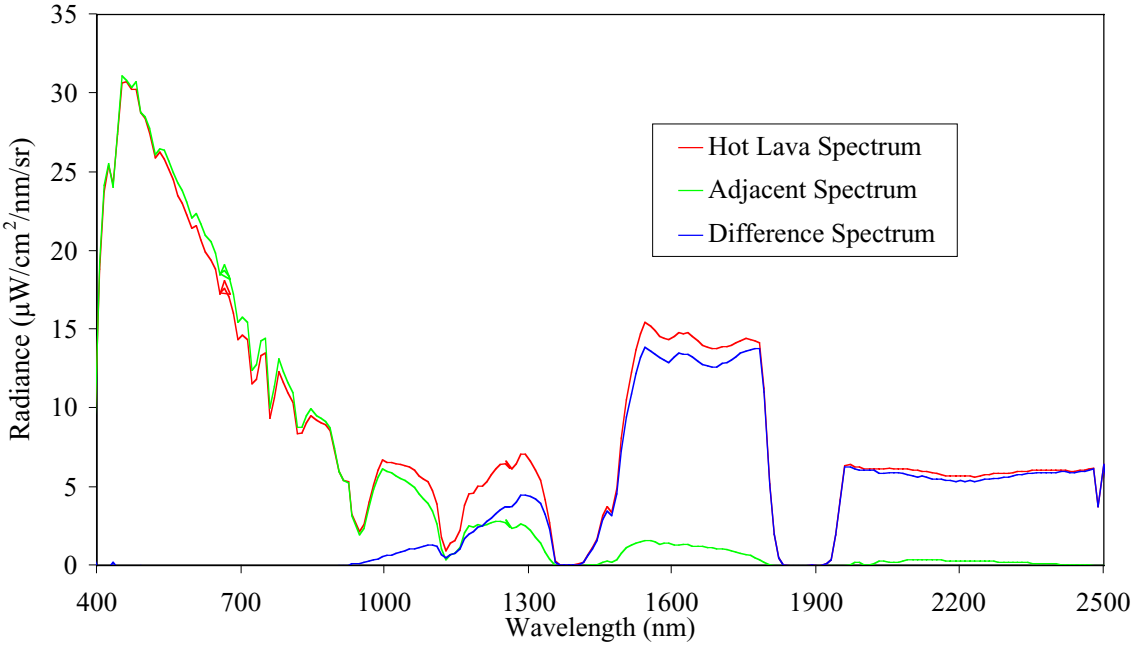

Figure 9. Spectra from hot lava target A, adjacent spectrum, and difference spectrum.

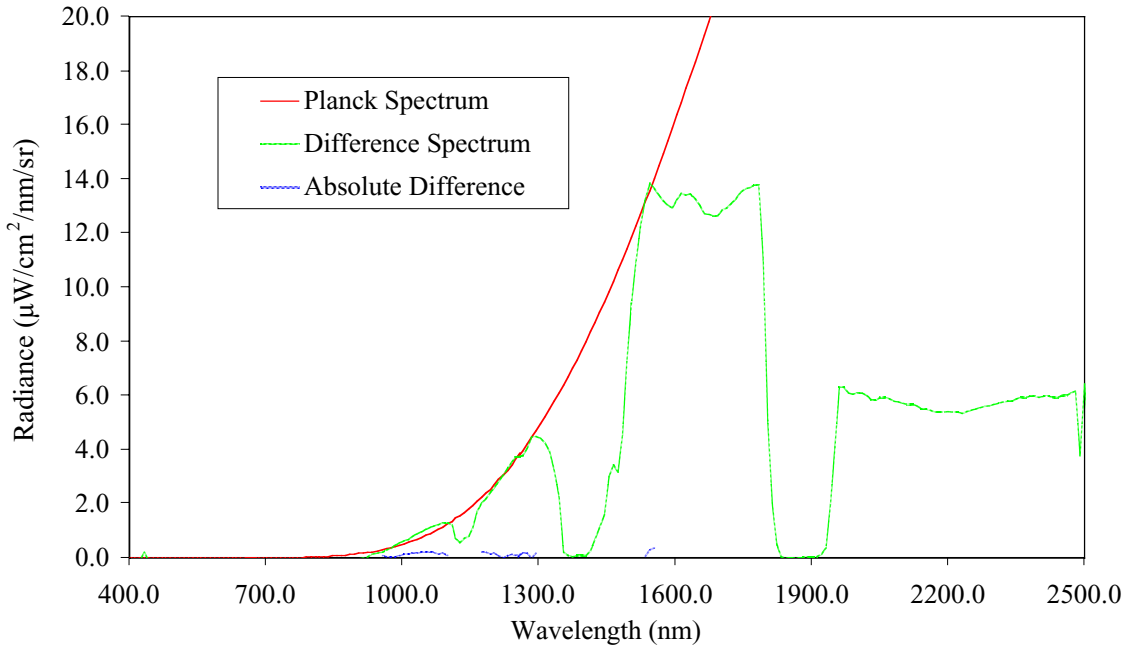

Figure 10. Fit of Planck function to AVIRIS spectrum for hot spot A with correction for solar reflected radiance. A temperature of 923˚K and area fraction of 0.24 was derived. The AVIRIS dynamic range is saturated in portions of the spectrum beyond 1500 nm.

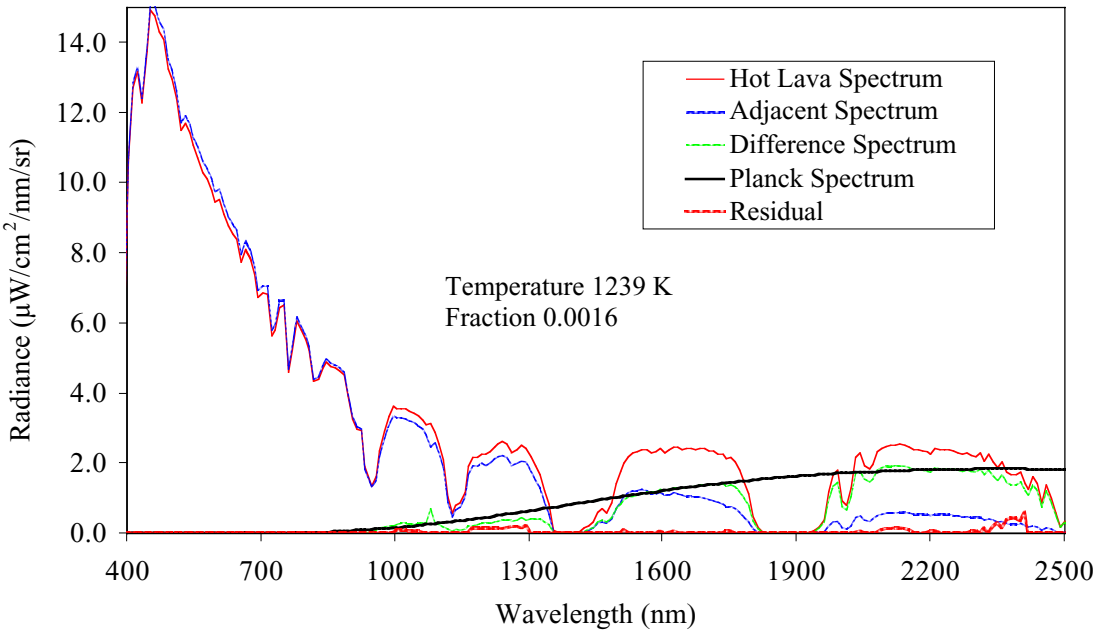

Figure 11. Spectral temperature and fractional area determination for hot spot C.

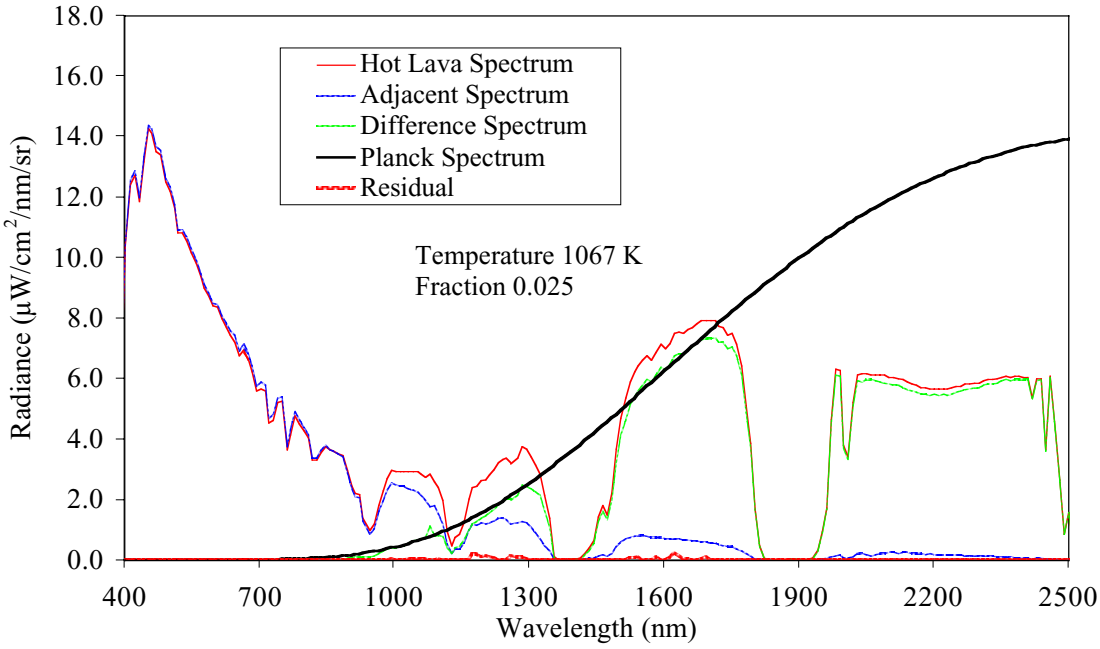

Figure 12. Spectral temperature and fractional area determination for hot spot E.

Table 1. Hawaii hot spot temperature and fractional fill determinations.

Site	Temperature (K)	Fractional Area
A	923	0.24
B	908	0.068
C	1239	0.0016
D	973	0.027
E	1067	0.025
F	1052	0.034
G	1168	0.0023

To further explore temperature and fractional area determinations with these AVIRIS measurements, a second form of spectral fitting algorithm was developed. Equation 2 gives the expression of the total radiance measured by AVIRIS used for this more sophisticated model based algorithm. In addition to the components given in Equation 1, the factor T_u is used to account for the upward attenuation of the lava emitted radiance and the factors F_2 and B_{t2} provide a second temperature target at the surface. This algorithm used the MODTRAN (Berk et al., 1989; Anderson et al., 1995, 2000) radiative transfer code to calculate the atmosphere and surface reflected radiance components as well as the one way transmittance for the emitted radiance from the surface to AVIRIS. To estimate the atmospheric radiance and surface reflected radiance, a MODTRAN spectrum was generated to fit the measured spectrum over the range 400 to 950 nm. For this fit the surface reflectance and visibility parameters were allowed to vary for the 5-km-visibility tropical atmospheric model until an optimal fit was achieved. MODTRAN was also used to calculate the transmittance from the surface to AVIRIS to account for attenuation of the surface emitted radiance. Figure 13 shows the extracted spectrum for hot spot C as well as the MODTRAN modeled spectrum calculated to match over the 400 to 950 nm range and the upward transmittance spectrum.

$$L_t = I_0\rho_a/\pi + I_0T_d\rho_sT_u/\pi + T_u(F_1B_{t1}+F_2B_{t2}) \qquad \text{Equation 2}$$

For temperature and fractional area analysis, the calculated MODTRAN spectrum was subtracted from the measured spectrum and the upward transmittance divided to generate a spectrum dominated by the hot target emitted radiance. The resulting corrected spectrum was fit with two Planck functions at two independent temperatures and fractional areas. Regions of near total atmospheric absorption were excluded from the fit. Figure 14 shows the fit for temperature and fractional area determination of hot spot C. The temperatures derived were 1283 K and 600 K at fractions fill areas of 0.0018 and 0.0033 respectively. The quality of the spectral fit is good with some residual disagreement near regions of atmospheric absorption. This more sophisticated algorithm more accurately models and compensates for the solar reflected and atmospheric attenuation factors in the estimation of surface lava temperature from the calibrated AVIRIS measurements. Future work is planned to refine the algorithm and model and further understand and minimize the effects of uncertainties in AVIRIS calibration and the MODTRAN radiative transfer calculations.

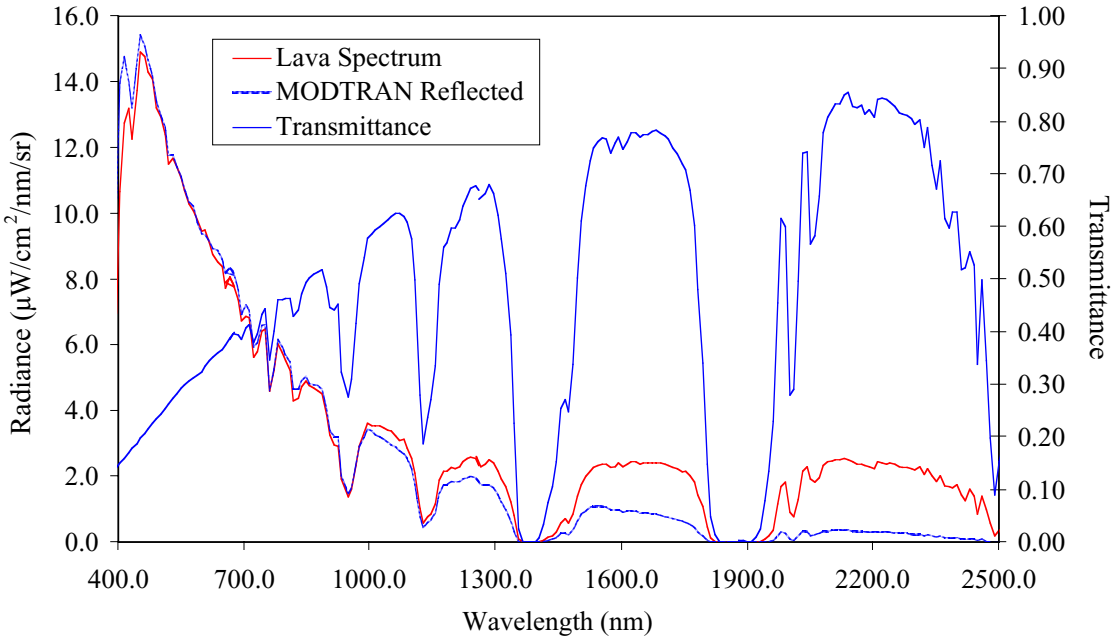

Figure 13. AVIRIS measured spectrum, MODTRAN modeled solar reflected spectrum and MODTRAN modeled upwards transmittance spectrum for hot lava target C.

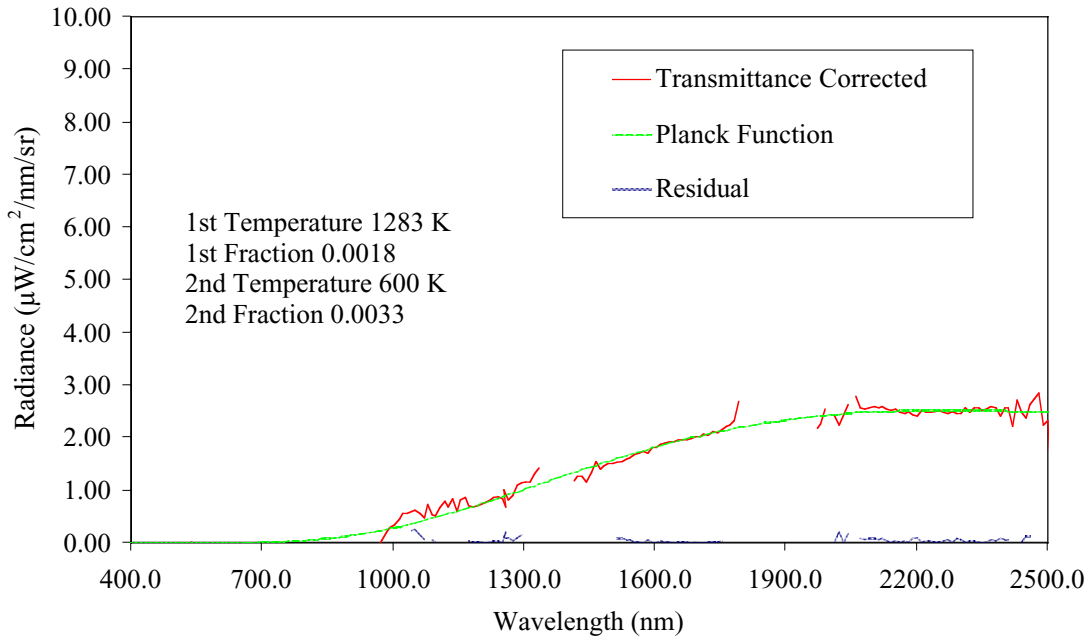

Figure 14. Spectral fit between two-Planck-function model and AVIRIS measured spectrum from hot lava target C with reflected solar radiance and atmospheric correction. Regions of strong atmospheric attenuation are excluded.

CONCLUSION

The AVIRIS imaging spectrometer measured the active volcanic vent region on the Big Island of Hawaii on April 26, 2000. Examination of the spectral image data set showed distinct expression of seven lava

hot spots. These hot spots show enhanced radiance signatures in the spectral region beyond 1000 nm with respect to all other Earth environment components in the AVIRIS data set. The full spectral shape measured by AVIRIS provided a basis for temperature and fractional area estimation from these hot spot spectra. An initial simple algorithm was used to estimate temperature and fractional area. This algorithm suppressed the solar reflected radiance in the hot lava spectrum by subtraction of an adjacent cool target spectrum. Following this correction, a spectral Planck-function model with both temperature and fractional area parameters was fitted to the corrected spectrum. The fit was restricted to spectral regions of high atmospheric transmittance and regions where the AVIRIS dynamic range was not saturated. Good spectral fits were achieved for the analyzed spectra from each of the seven lava hot spots. Derived temperatures ranged from 923 K to 1239 K and fractional areas from 0.0016 to 0.24.

A second temperature estimation algorithm was implemented that used the calculations by the MODTRAN radiative transfer code. This algorithm used MODTRAN to estimate the solar reflected component in the measured spectrum as well as the atmospheric transmittance from the surface to AVIRIS. With these MODTRAN-based corrections more of the spectral range of the measured spectrum was usable for fitting. In conjunction with these more advanced corrections, a two-Planck-function model with independent temperatures and fractional area was used. When applied to lava hot spot C, temperatures of 1283 K and 600 K (and respective fractional areas of 0.0018 and 0.0033) were derived. This more sophisticated temperature and fractional-area estimation algorithm more fully accounts for the complexity of the surface and atmospheric components expressed in the measured hot lava spectrum.

These analyses and results demonstrate the use of full solar reflected spectrum imaging spectrometer measurements for hot target temperature and fractional area estimation. The results are tied to the spectral shape of the measured radiance as well as the intensity. Accounting for both spectral shape and intensity is required to avoid the ambiguity between intensity and fractional-area fill. Imaging spectrometer measurements enable a direct approach, based in fundamental physics rather than data statistics, to derive these important properties of hot targets from the remote sensing perspective.

REFERENCES

Anderson, G. P., J. Wang, and J. Chetwynd, "An Update and Recent Validations Against Airborne High Resolution Interferometer Measurements," *Summaries of the Fifth Annual JPL Airborne Earth Science Workshop*, JPL Pub. 95-1, Vol. 1, *AVIRIS Workshop*, Jet Propulsion Laboratory, Pasadena, California, pp. 5–8, January 23, 1995.

Anderson, G. P., A. Berk, P. K Acharya, M. W. Mathew, L. S. Bernstein, J. H. Chetwynd, H. Dothe, S. M. Adler-Golden, A. Ratkowski, G. W. Felde, J. A. Gardner, M. L. Hoke, S. C. Richtsmeir, B. Pukall, J. Mello, and L. S. Jeong, "MODTRAN4: Radiative transfer modeling for remote sensing," in *Proceedings SPIE, Algorithms for Multispectral, Hyperspectral, and Ultraspectral Imagery VI*, Vol. 4049, S. S. Shen and M. R. Descour, eds., pp. 176–183, 2000.

Berk, A., L. S. Bernstein, and D. C. Robertson, *MODTRAN: A Moderate Resolution Model for LOWTRAN 7*, Final report, GL-TR-0122, AFGL, Hanscomb AFB, Massachusetts, 42 pp., 1989.

Chrien, T. G., R. O. Green, and M. L. Eastwood, "Accuracy of the spectral and radiometric laboratory calibration of the Airborne Visible/Infrared Imaging Spectrometer (AVIRIS)," *SPIE Vol. 1298, Imaging spectroscopy of the terrestrial environment*, G. Vane, ed., pp. 37–49, 1990.

Chrien, T. G., R. O. Green, C. Chovit, M. Eastwood, J. Faust, P. Hajek, H. Johnson, H. I. Novack, and C. Sarture, "New Calibration Techniques for the Airborne Visible/Infrared Imaging Spectrometer

(AVIRIS), 1995," *Proc. Fifth Annual Airborne Earth Science Workshop*, JPL Pub. 95-1, Jet Propulsion Laboratory, Pasadena, California, pp. 33–34, 1995.

Chrien, T. G., R. O. Green, C. J. Chovit, M. L. Eastwood, and C. M. Sarture, "Calibration of the Airborne Visible/Infrared Imaging Spectrometer in the Laboratory," *Proc. Sixth Annual Airborne Earth Science Workshop*, JPL Pub. 96-4, Vol. 1, Jet Propulsion Laboratory, Pasadena, California, pp. 39–48, March 3–5, 1996.

Chrien, T. G., R. O. Green, B. Pavri, and J. Wall, "Calibration Validation of the AVIRIS Portable Radiance Standard," *Proc. Ninth Airborne Earth Science Workshop*, JPL Pub. 00-18, Jet Propulsion Laboratory, Pasadena, California, pp. 101–110, 2000.

Green, R. O., "Estimation of Biomass Fire Temperature and Areal Extent from Calibrated AVIRIS Spectra," Proc. Sixth Annual Airborne Earth Science Workshop, Jet Propulsion Laboratory, JPL Pub. 96-4, Vol. 1, pp. 105–113, March 3-5, 1996.

Green, R. O., M. L. Eastwood, C. M. Sarture, T. G. Chrien, M. Aronsson, B. J. Chippendale, J. A. Faust, B. E. Pavri. C. J. Chovit, M. Solis, M. R. Olah, and Q. Williams, "Imaging spectroscopy and the Airborne Visible/Infrared Imaging Spectrometer (AVIRIS)," *Remote Sens Environ* 65: (3) 227–248, Sept. 1998.

Liou, K. N., *An Introduction to Atmospheric Radiation*, Academic Press, Inc., New York, pp. 392, 1980.

Oppenheimer, C., D. A. Rothery, D. C. Pieri, M. J. Abrams, V. Carrere, "Analysis of Airborne Visible/Infrared Imaging Spectrometer (AVIRIS) Data of Volcanic Hot-Spots," Open Univ., Dept. Earth Sci./Milton Keynes/MK7 6AA/Bucks./ENGLAND/*International Journal of Remote Sensing*, 14, (16), 2919–2934, 1993.

ACKNOWLEDGEMENTS

The research described herein was carried out at the Jet Propulsion Laboratory, California Institute of Technology, under a contract with the National Aeronautics and Space Administration.

Reference herein to any specific commercial product, process, or service by trade name, trademark, manufacturer, or otherwise, does not constitute or imply its endorsement by the United States Government or the Jet Propulsion Laboratory, California Institute of Technology.